Single-spin asymmetries in e-p scattering with intermediate state resonances

Peter Blunden (University of Manitoba)

Positron Working Group Workshop

March 2024

Collaborators: Jaseer Ahmed and Wally Melnitchouk

Outline

- Single spin asymmetries (SSA): beam normal B_n and target normal A_n cases: absorptive **imaginary** part of two-photon exchange (TPE)
  - What can we learn from B_n vs A_n?
  - What are the prospects for measuring A_n at JLab?
- Relationship to TPE calculations for elastic e-p scattering cross sections and the ratio G_E/G_M : dispersive **real** part of TPE
- Real and Imaginary parts connected by dispersion relations

Dispersive method

Unitarity → $$\mathrm{Im}\langle f|\mathcal{M}|i\rangle \sim \sum_n \int dW_n\, dQ_1^2\, dQ_2^2\ \langle f|\mathcal{M}^*|n\rangle\langle n|\mathcal{M}|i\rangle$$

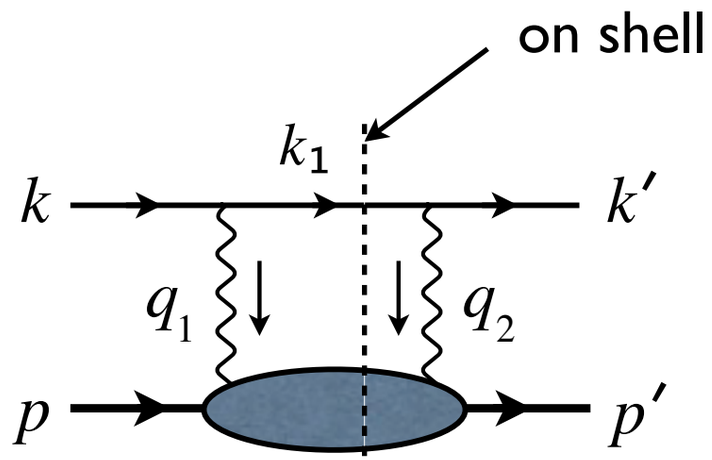

- Imaginary part determined by unitarity
- Uses only on-shell form factors (or helicity amplitudes), directly fit to data
- Real part determined from dispersion relations

- Resonance intermediate states:

$$\Delta(1232)3/2^+,\ N(1440)1/2^+,\ N(1520)3/2^-,\ N(1535)1/2^-,$$
$$\Delta(1620)1/2^-,\ N(1650)1/2^-,\ \Delta(1700)3/2^-,\ N(1710)1/2^+,\ N(1720)3/2^+$$

- Use CLAS exclusive meson electroproduction data for helicity amplitudes

$$A_{1/2},\ A_{3/2},\ S_{1/2}$$

- Include Breit-Wigner lineshape

CLAS helicity amplitudes: examples of data

Δ(1232)

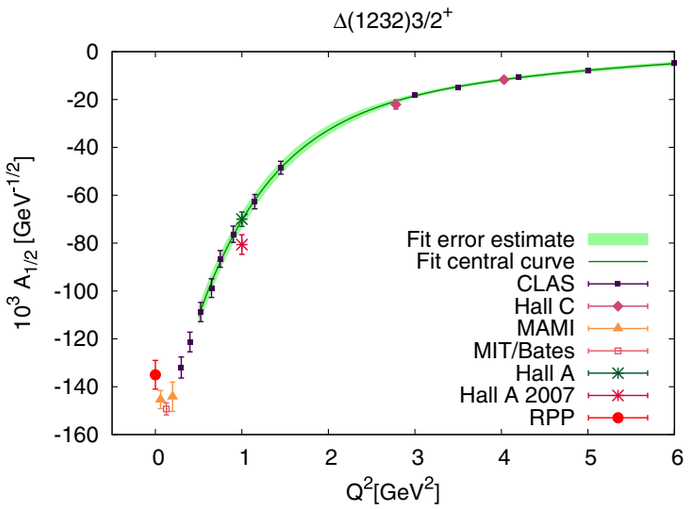

(a)

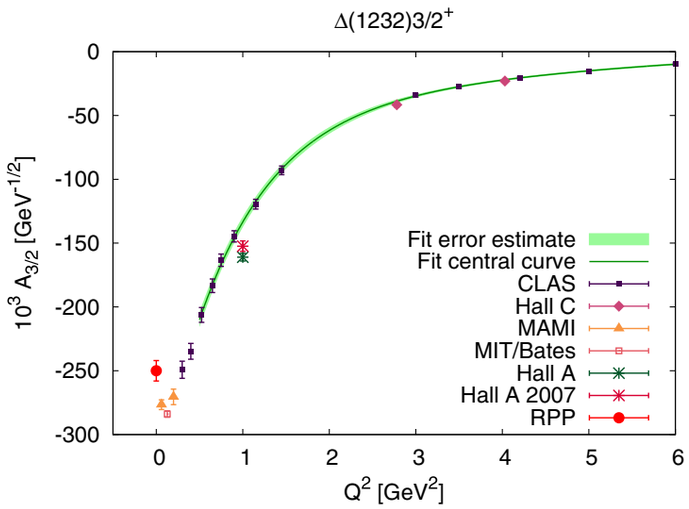

(b)

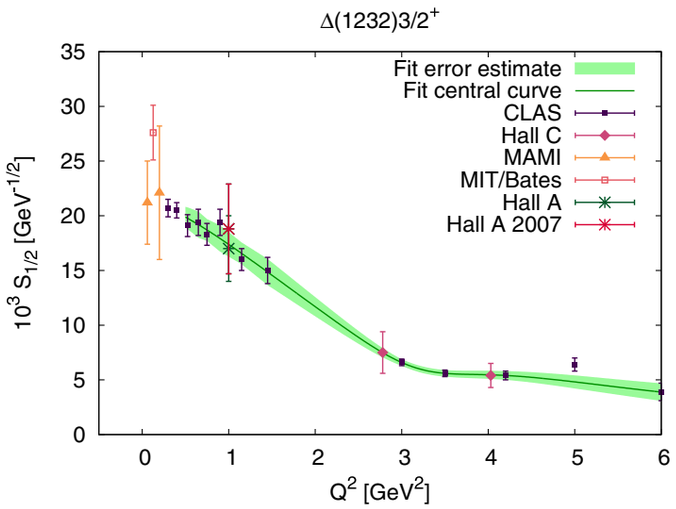

(c)

N(1440)

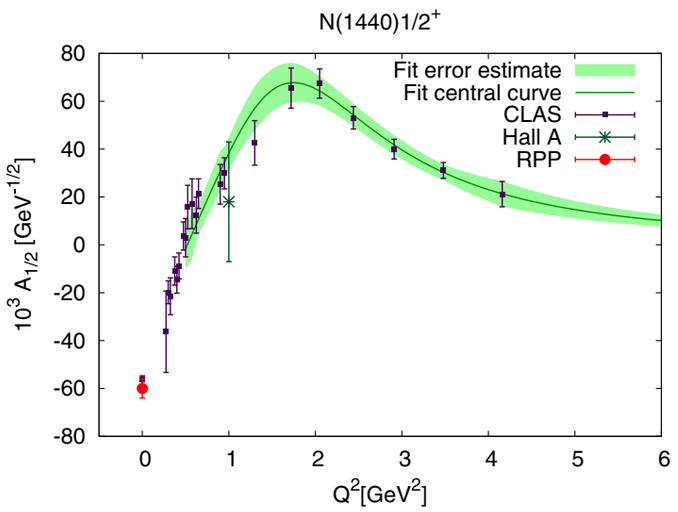

(d)

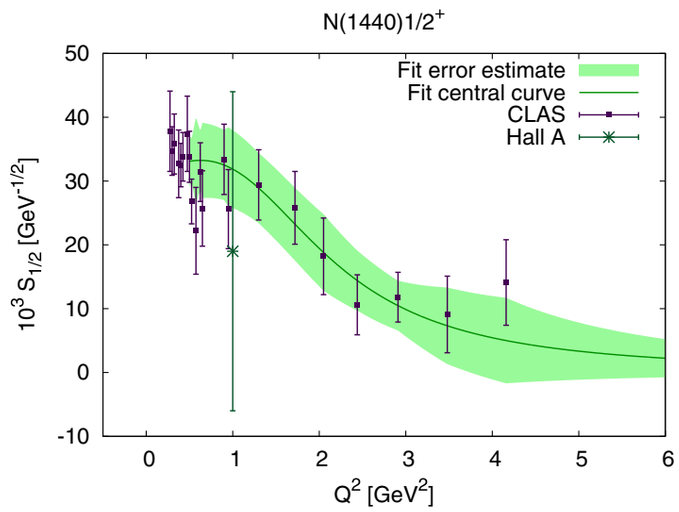

(e)

Hiller Blin *et al.*, PRC **100**, 035201 (2019)

N(1520)

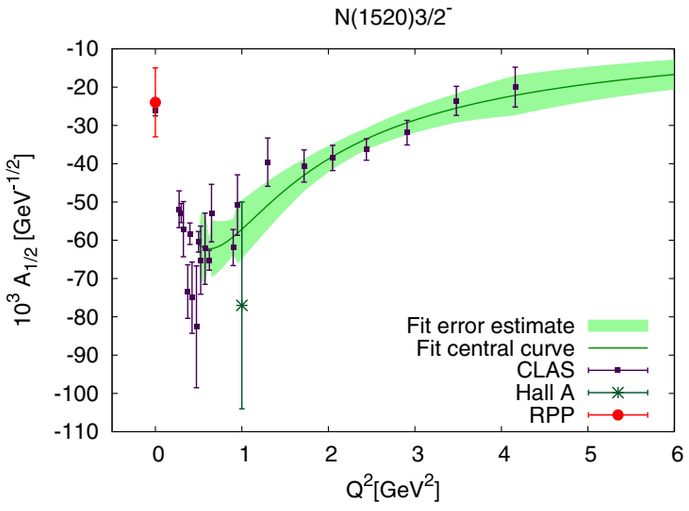

(f)

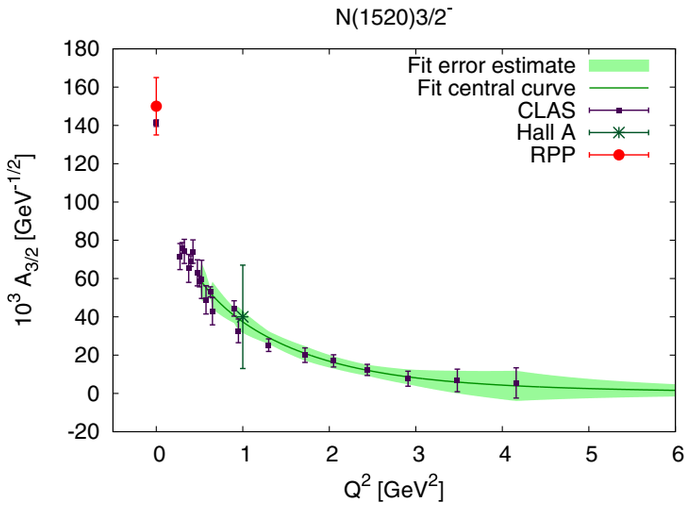

(g)

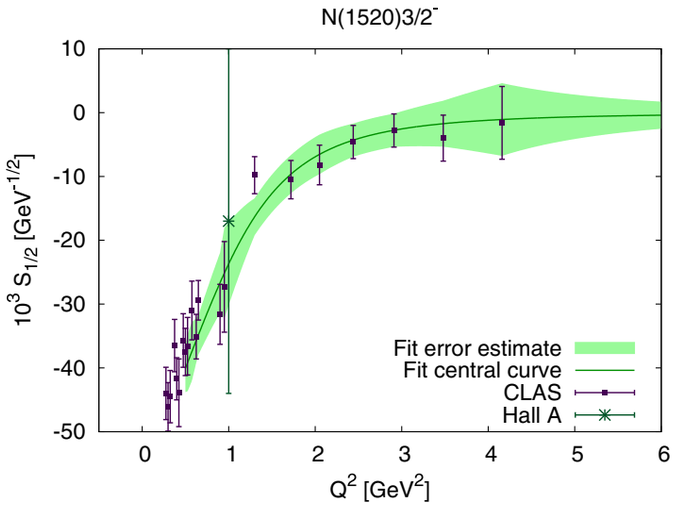

(h)

CLAS unpolarized cross sections vs W^2

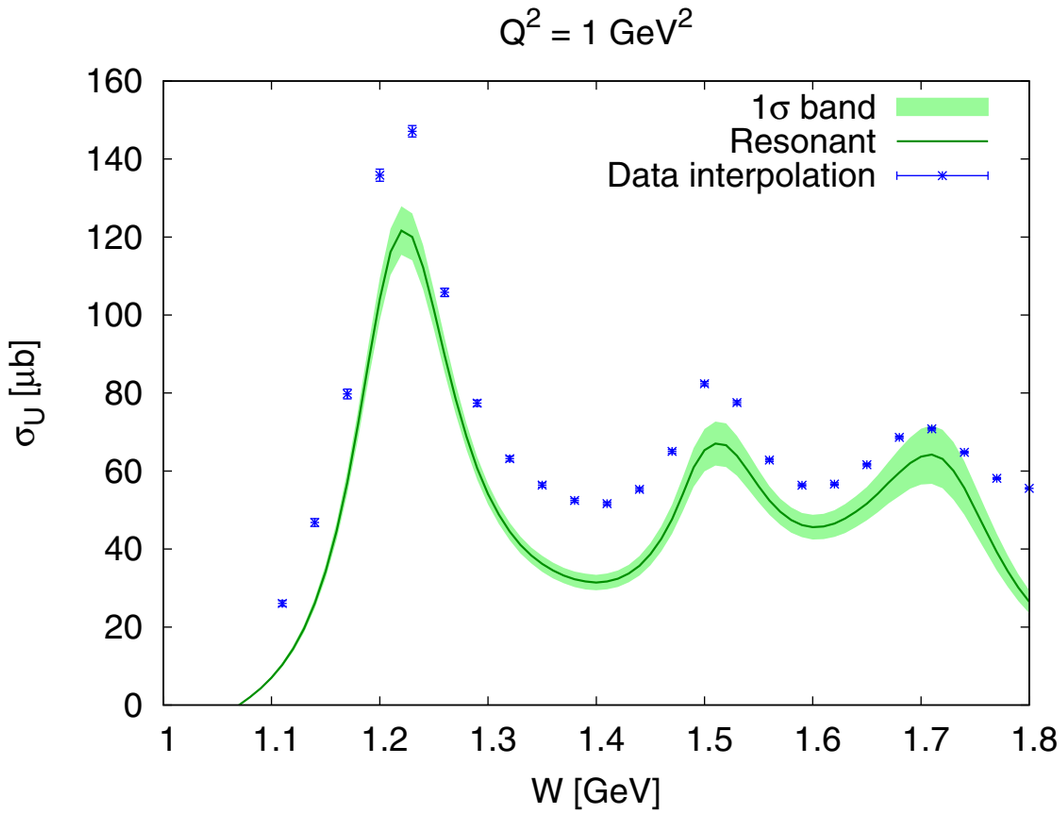

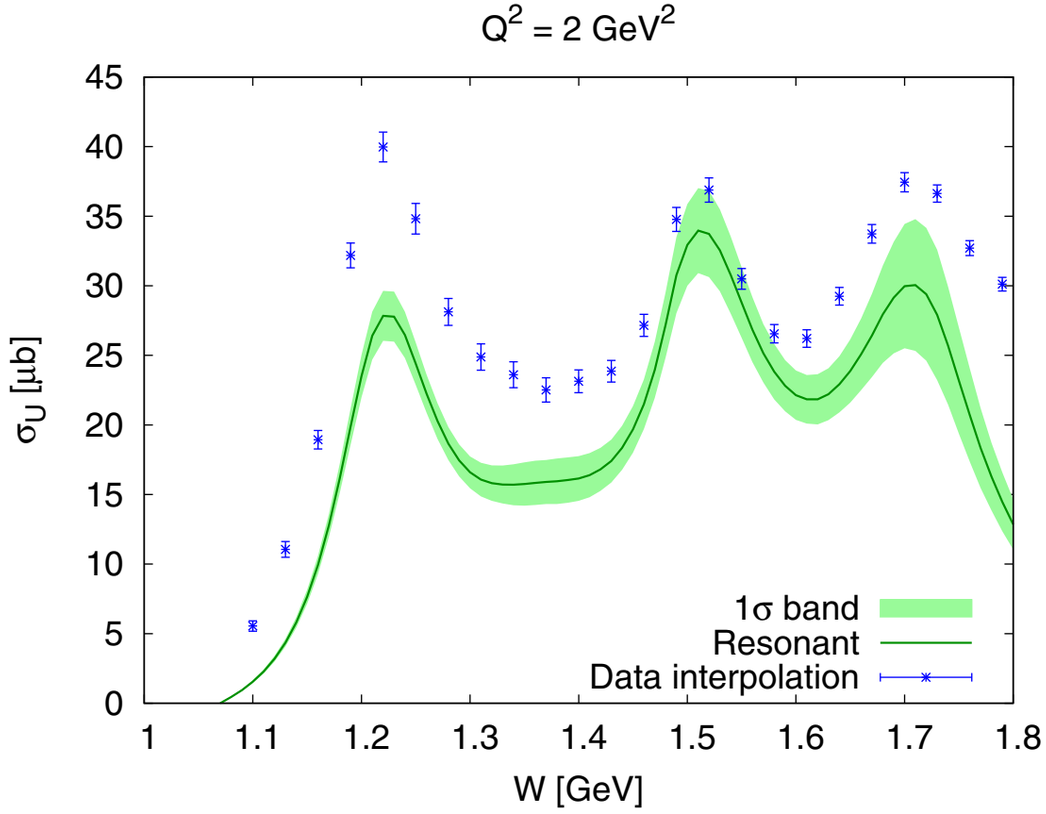

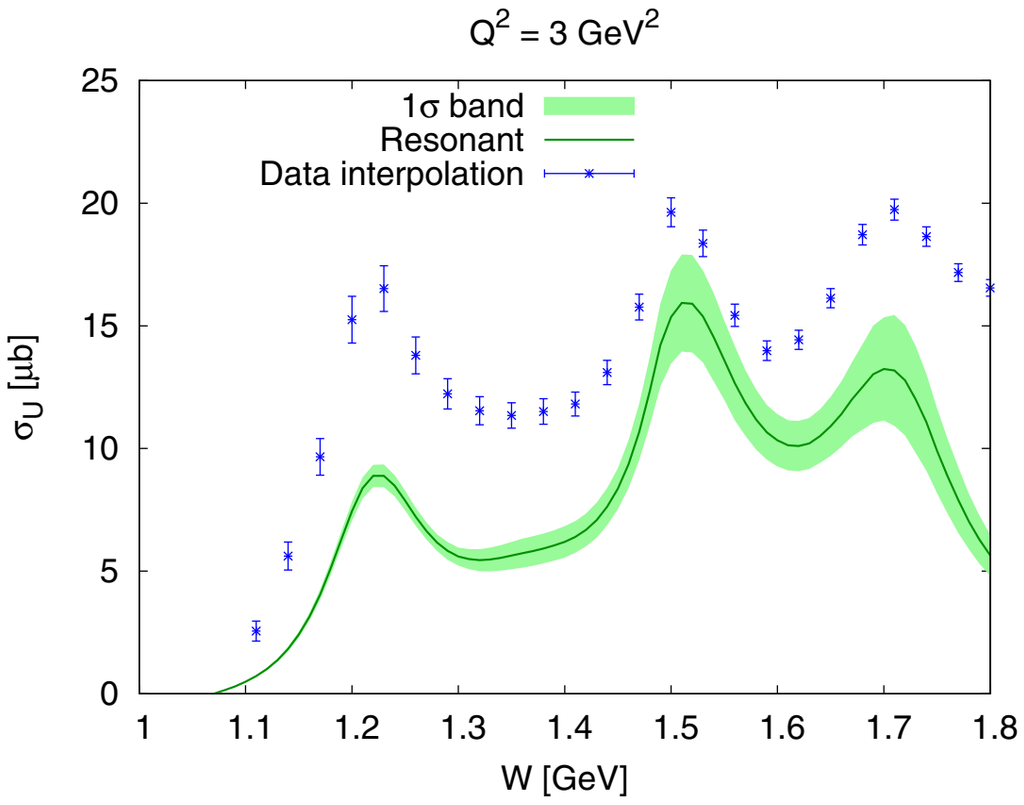

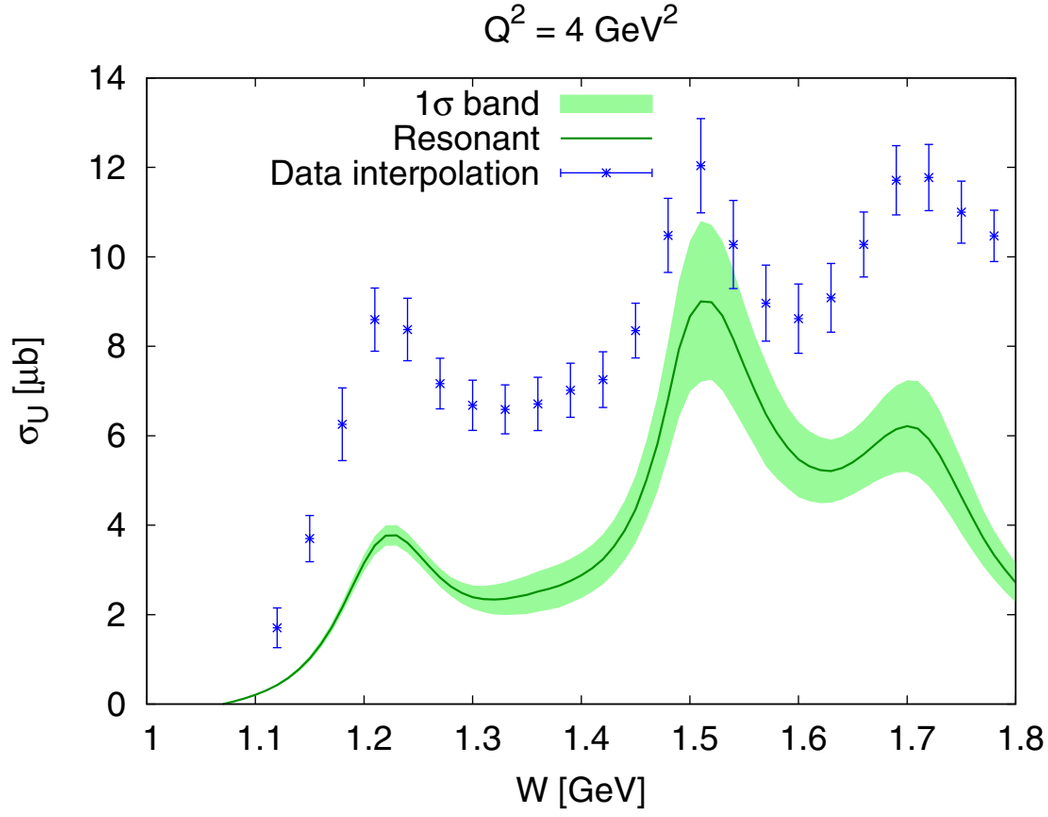

- Resonant vs. Total cross section at increasing Q^2

TPE using dispersion relations

Generalized form factors

$$\mathcal{M}_{\gamma\gamma} \to (\gamma_\mu)^{(e)} \otimes \left(F_1'(Q^2,\nu)\gamma^\mu + F_2'(Q^2,\nu)\frac{i\sigma^{\mu\nu}q_\nu}{2M} \right)^{(p)}$$
$$+ (\gamma_\mu\gamma_5)^{(e)} \otimes \left(G_a'(Q^2,\nu)\gamma^\mu\gamma_5 \right)^{(p)}$$

Dispersion relations

$$\mathrm{Re}\ F_1'(Q^2,\nu) = \frac{2}{\pi}\mathcal{P}\int_{-\tau}^{\infty} d\nu'\ \frac{\nu}{\nu'^2-\nu^2}\,\mathrm{Im}\ F_1'(Q^2,\nu')\,,$$
$$\mathrm{Re}\ F_2'(Q^2,\nu) = \frac{2}{\pi}\mathcal{P}\int_{-\tau}^{\infty} d\nu'\ \frac{\nu}{\nu'^2-\nu^2}\,\mathrm{Im}\ F_2'(Q^2,\nu')\,,$$
$$\mathrm{Re}\ G_a'(Q^2,\nu) = \frac{2}{\pi}\mathcal{P}\int_{-\tau}^{\infty} d\nu'\ \frac{\nu'}{\nu'^2-\nu^2}\,\mathrm{Im}\ G_a'(Q^2,\nu')\,.$$

Integral extends into ``unphysical region'' down to zero energy ($\cos\theta < -1$)

Direct measurements of Im part

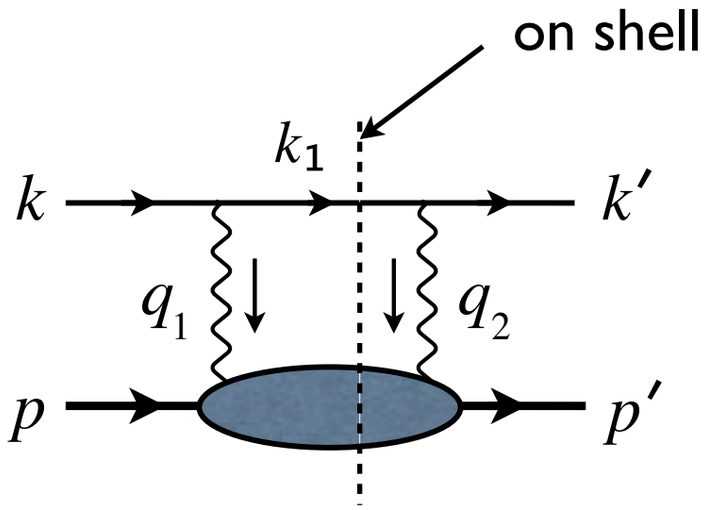

This is all in the physical region.

Beam normal spin asymmetry: additional dependence on spin-flip FFs

$$B_n = -\frac{m_e}{M}\sqrt{2\epsilon(1-\epsilon)(1+\tau)}\,\frac{1}{\sigma_R}\mathrm{Im}\left\{-G_M G_a' + G_E F_4' + \nu F_1 F_5'\right\}$$

Target normal spin asymmetry: same generalized FFs as cross section

$$A_n = \sqrt{2\epsilon(1+\epsilon)\tau}\,\frac{1}{\sigma_R}\mathrm{Im}\left\{-G_M(F_1' - \tau F_2') + G_E\left(F_1' + F_2' + \frac{1+\tau}{\nu}G_a'\right)\right\}$$

Probe different aspects of TPE!

TPE correction to cross section:

$$\delta_{\gamma\gamma} = \frac{1}{\sigma_R}\mathrm{Re}\left\{\epsilon G_E(F_1' - \tau F_2') + G_M\left(\tau(F_1' + F_2') + \nu(1-\epsilon)G_a'\right)\right\}$$

Ingredients of the calculation

$$\mathrm{SSA} = -\frac{\alpha\, Q^2}{\pi D(s,Q^2)} \int_{M^2}^{W^2_{\max}} dW^2\, \frac{|\vec{k}_1|}{4\sqrt{s}} \int_{-1}^{1} d\cos\theta_{k_1} \int_0^{2\pi} d\phi_{k_1}\, \frac{\mathrm{Im}\, L_{\rho\mu\nu} H^{\rho\mu\nu}}{Q_1^2\, Q_2^2}.$$

Kinematic bounds on Q_1^2 and Q_2^2

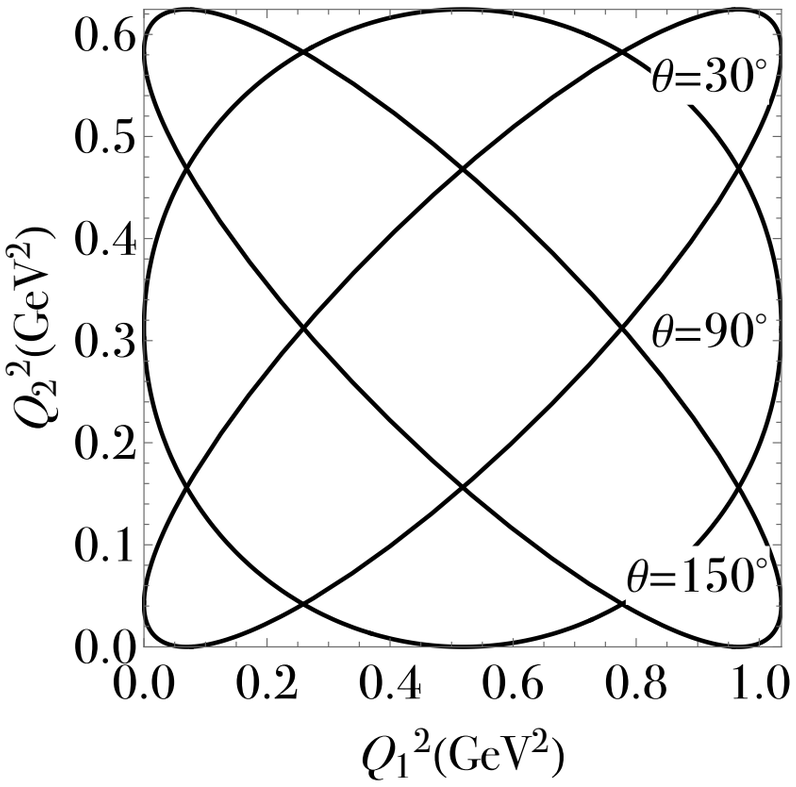

$Q^2_1 \simeq 0,\ Q^2_2 \neq 0$

↓

$k \,//\, k_1$

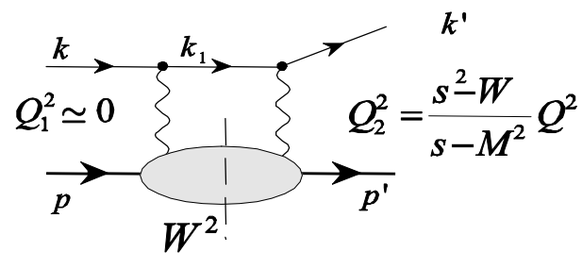

Quasi - VCS

$Q^2_1 \neq 0,\ Q^2_2 \simeq 0$

↓

$k_1 \,//\, k'$

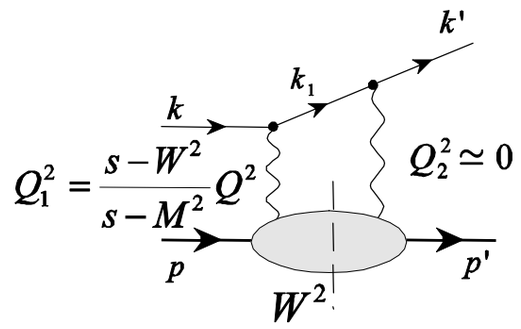

Quasi - VCS

$Q^2_1 \simeq 0,\ Q^2_2 \simeq 0$

↓

$k_1 = 0,\ W = \sqrt{s} - m_e$

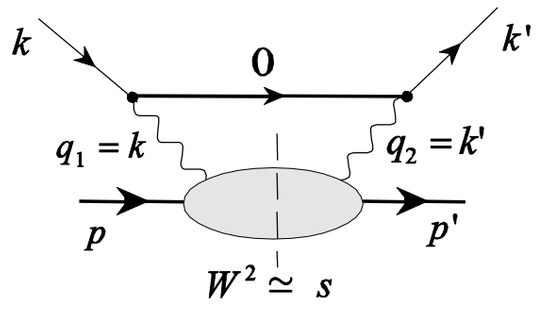

Quasi - RCS

Kinematic enhancement for QRCS in B_n

- Pasquini & Vanderhaeghen (2004)
- Afanasev & Merenkov (2004)

Quasi-Real Compton Scattering (QRCS)

$$\mathrm{SSA} = -\frac{\alpha\, Q^2}{\pi D(s,Q^2)} \int_{M^2}^{W^2_{\max}} dW^2\, \frac{|\vec{k}_1|}{4\sqrt{s}} \int_{-1}^{1} d\cos\theta_{k_1} \int_0^{2\pi} d\phi_{k_1}\, \frac{\mathrm{Im}\, L_{\rho\mu\nu} H^{\rho\mu\nu}}{Q_1^2\, Q_2^2}.$$

- Quasi-singular behaviour as $\mathrm{W} \to \mathrm{W}_{\max}$
- Two hard collinear photons
- Analogous to real Compton scattering

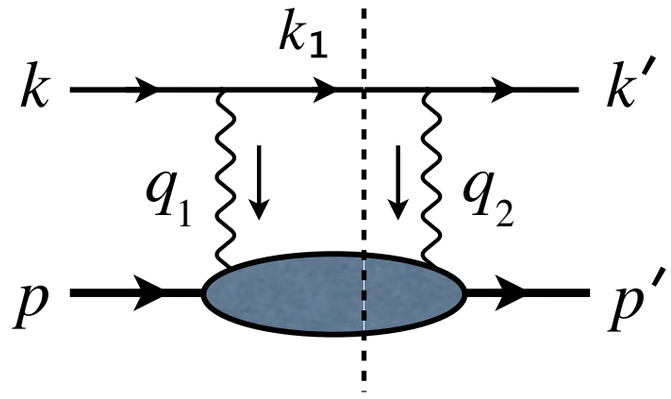

$$W_{\max} = \sqrt{s} - m_e, \quad E_{k_1} = m_e, \quad |\vec{k}_1| = 0$$

$$\text{At } W = W_{\max}: \qquad Q_1^2 = Q_2^2 = m_e \frac{W^2_{\max} - M^2}{\sqrt{s}}$$

- Slowly varying numerator and rapidly varying denominator for $\mathrm{W} \sim \mathrm{W}_{\max}$
- Strategy: numerator evaluated at $Q_1^2 = Q_2^2 = 0$ times

$$\frac{|\vec{k}_1|}{4\sqrt{s}} \int d\Omega_{k_1} \frac{1}{Q_1^2\, Q_2^2}$$

- This integral can be done analytically.
- Match to numerical solution for W below $\mathrm{W}_{\max}$

Quasi-Real Compton Scattering (QRCS)

Example above nominal threshold for N(1520)

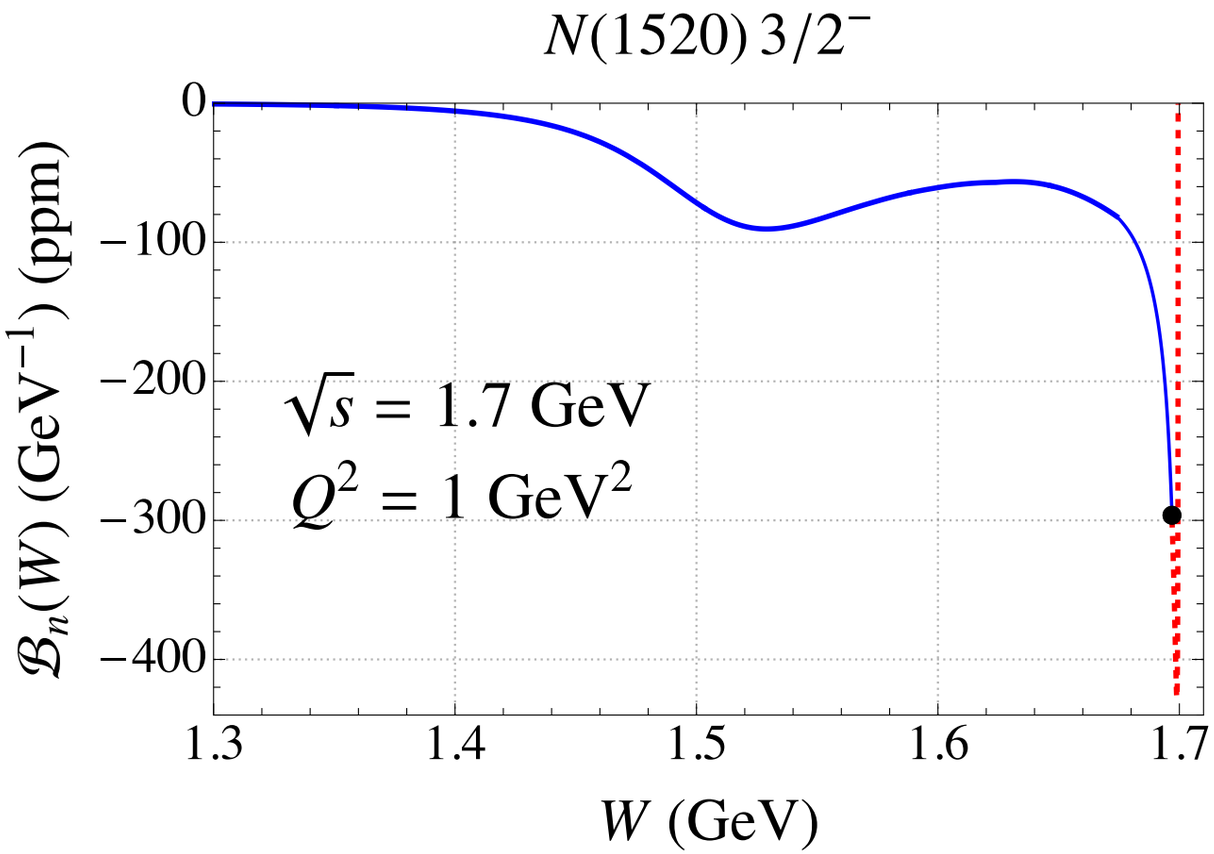

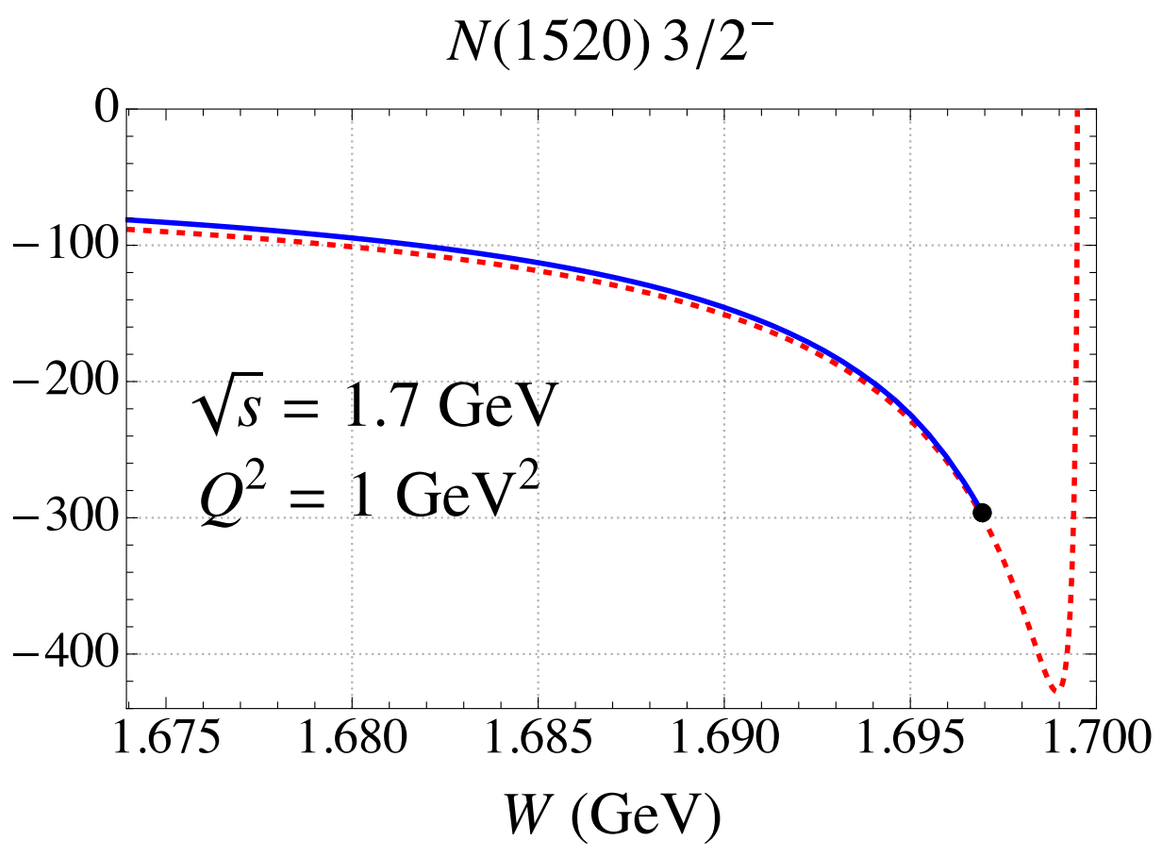

$$B_n = \int_{W_{\rm th}}^{W_{\rm max}} dW\ \mathcal{B}_n(W)$$

Match to numerical solution at $W^2 = \sqrt{s} - 5m_e$

Beam normal SSA: fixed E vs θ

Ahmed, Blunden, Melnitchouk, PRC **108**, 055202, (2023)

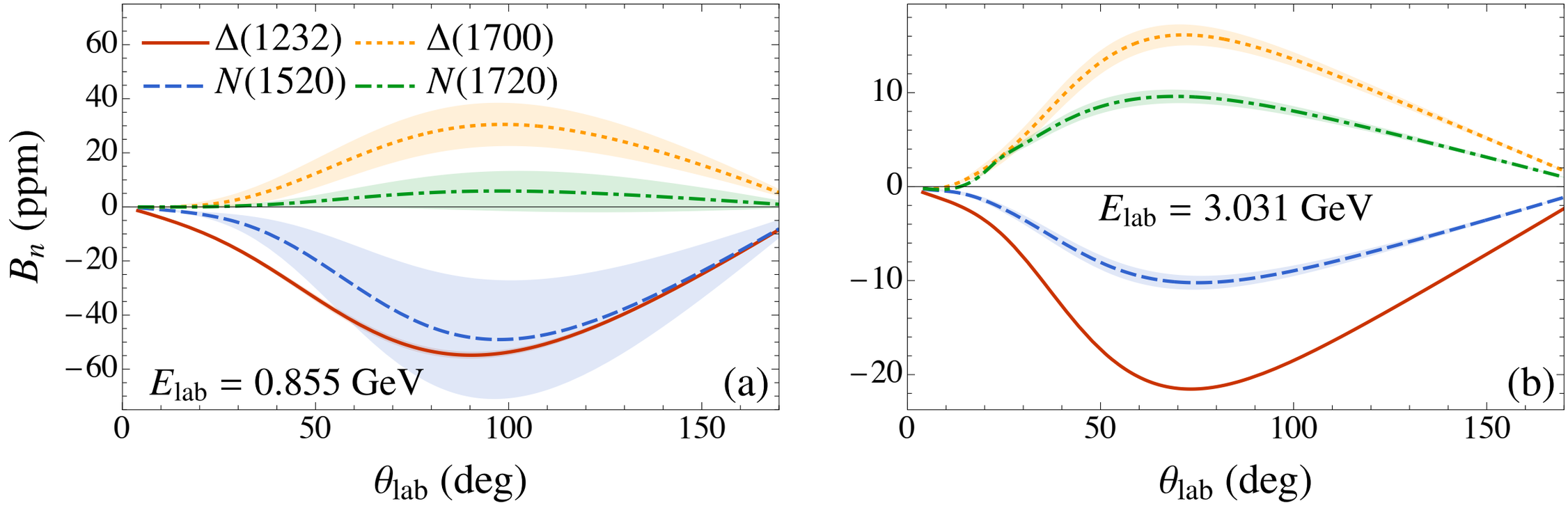

- Individual contributions from four largest spin $3/2$ resonances
- Decreases as E increases
- Spin $1/2$ contributions suppressed by an order of magnitude
- Significant cancellation between positive parity ($\Delta(1232)$, $N(1520)$) and negative parity ($\Delta(1700)$, $N(1720)$) resonances

Beam normal SSA: fixed E vs θ

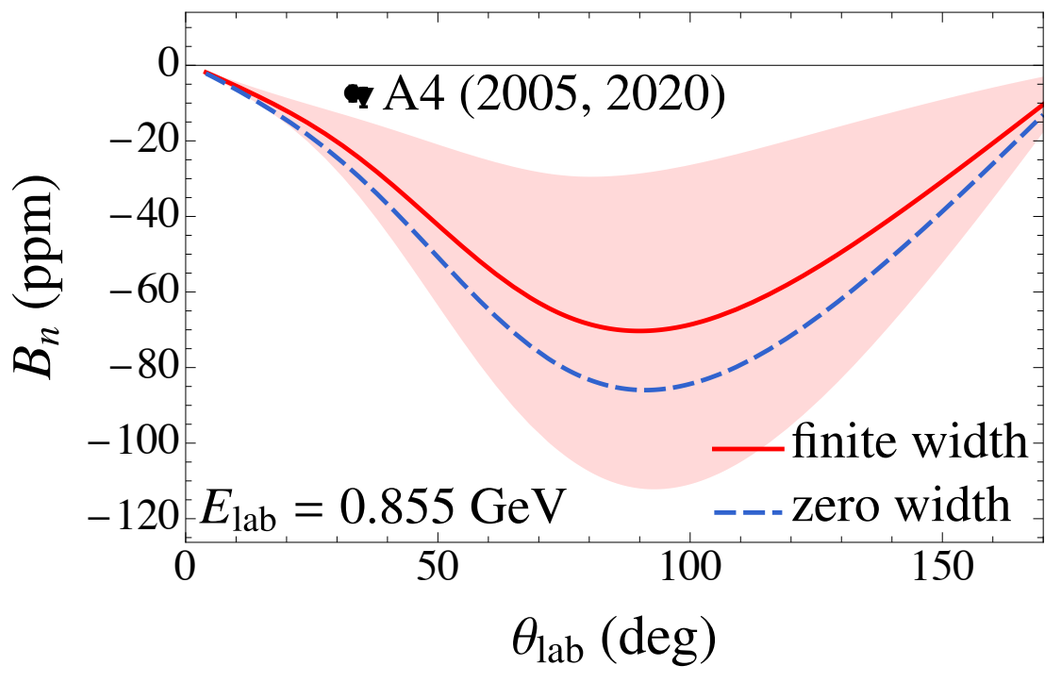

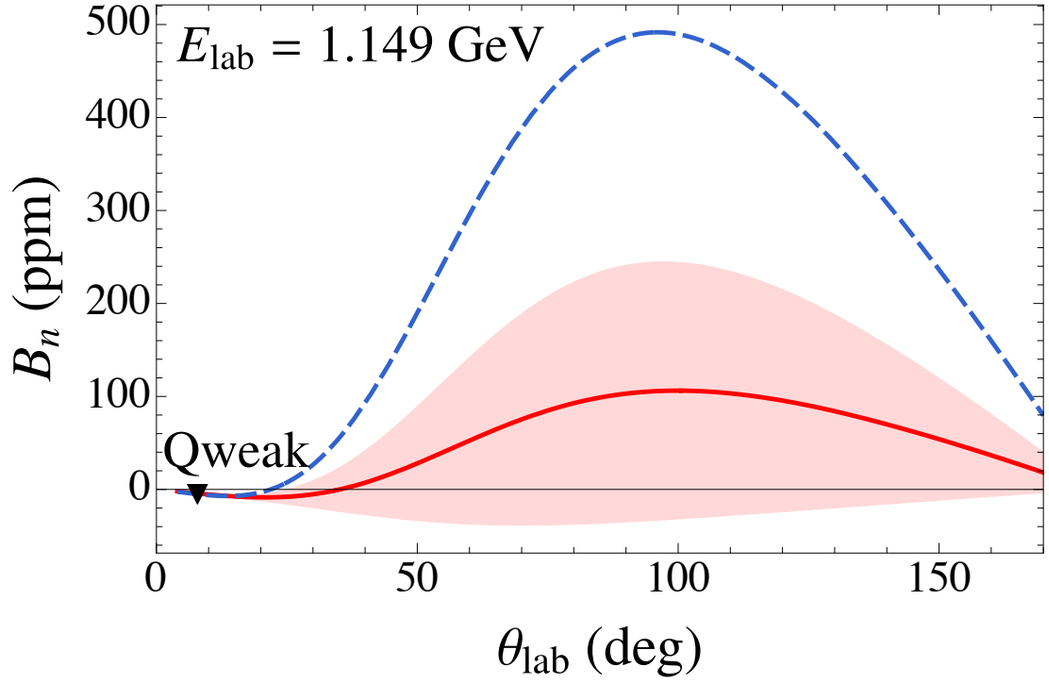

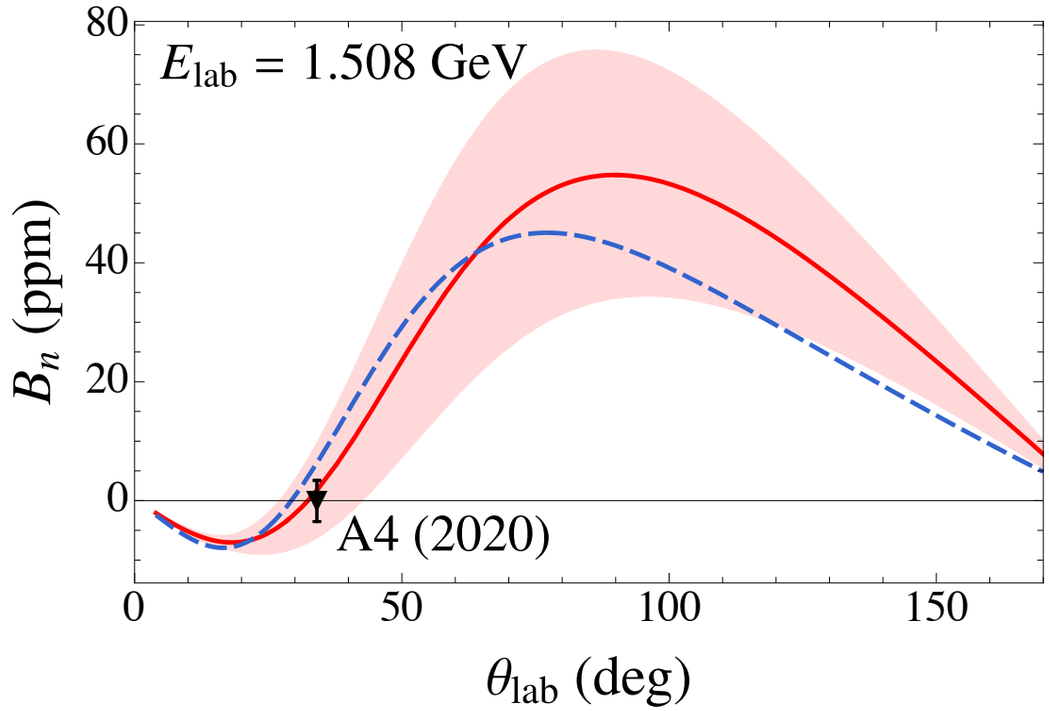

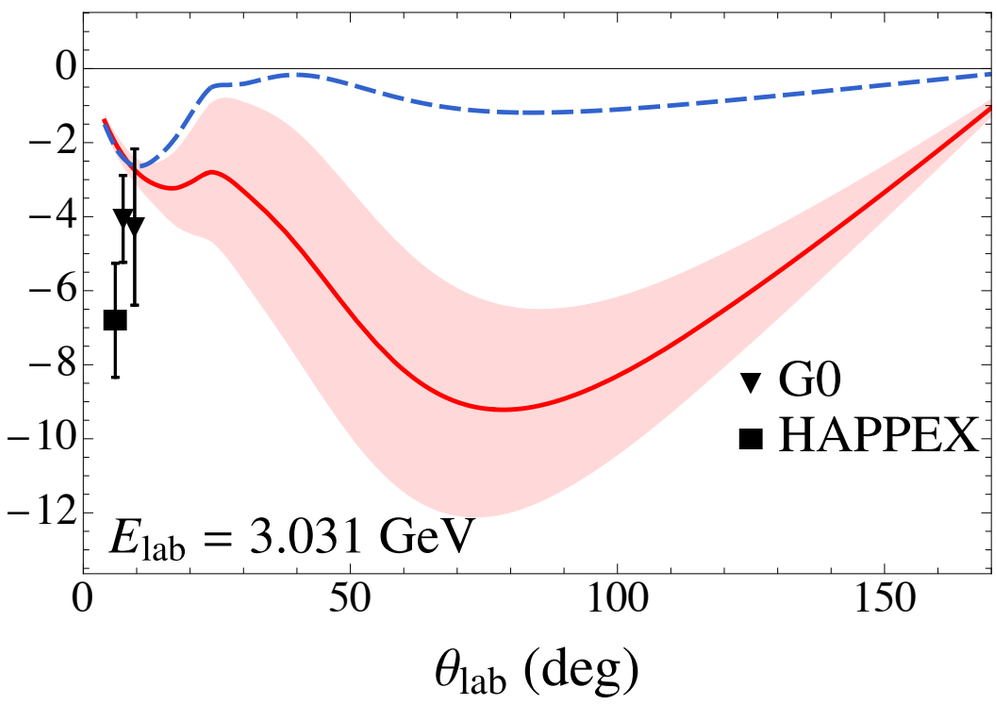

- Tends to overshoot data at low energies and forward angles
- Tends to undershoot data at high energies and forward angles

Qweak data point magnified

- Afanasev & Merenkov (2004)
- Pasquini & Vanderhaeghen (2004)
- Gorchtein (2006)

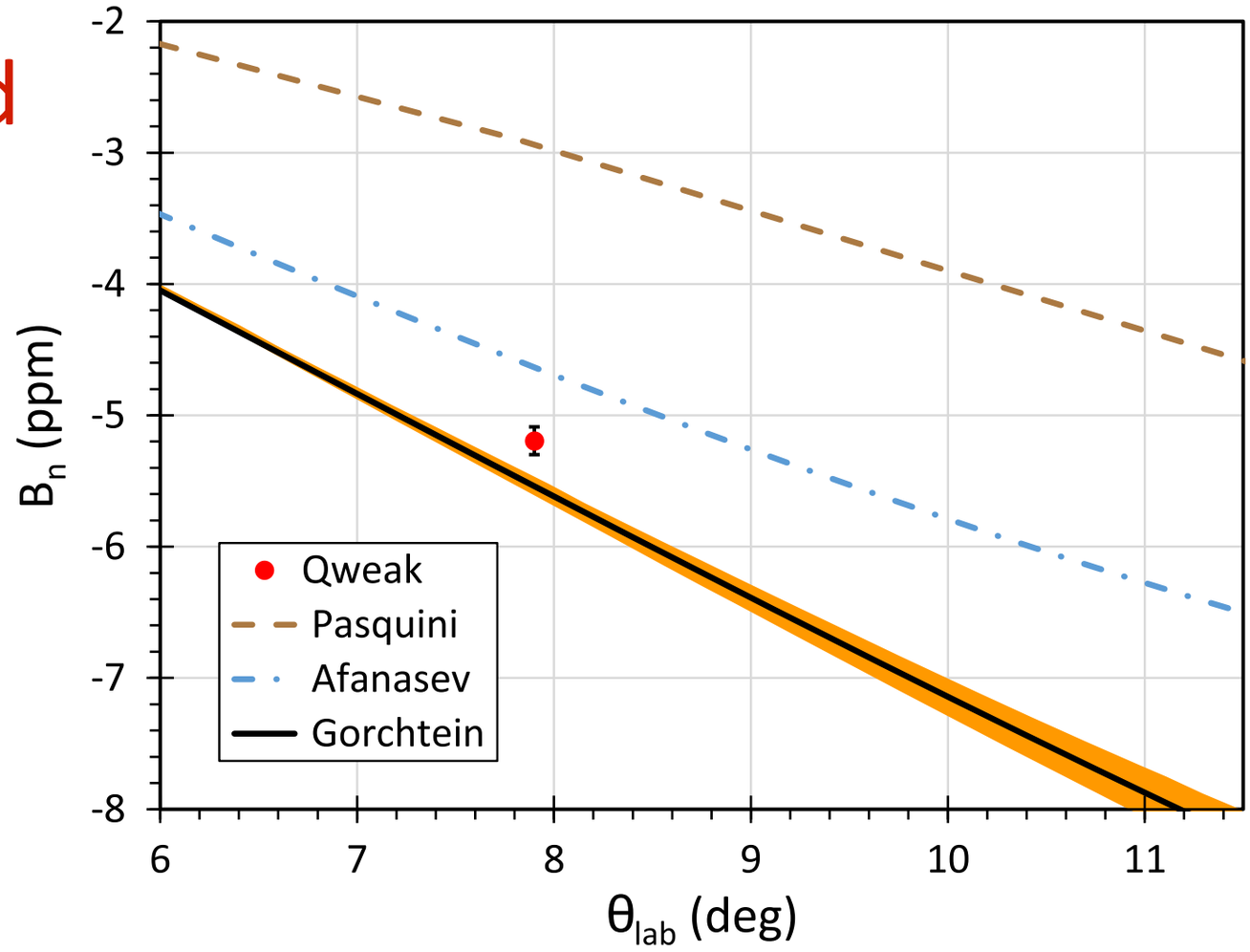

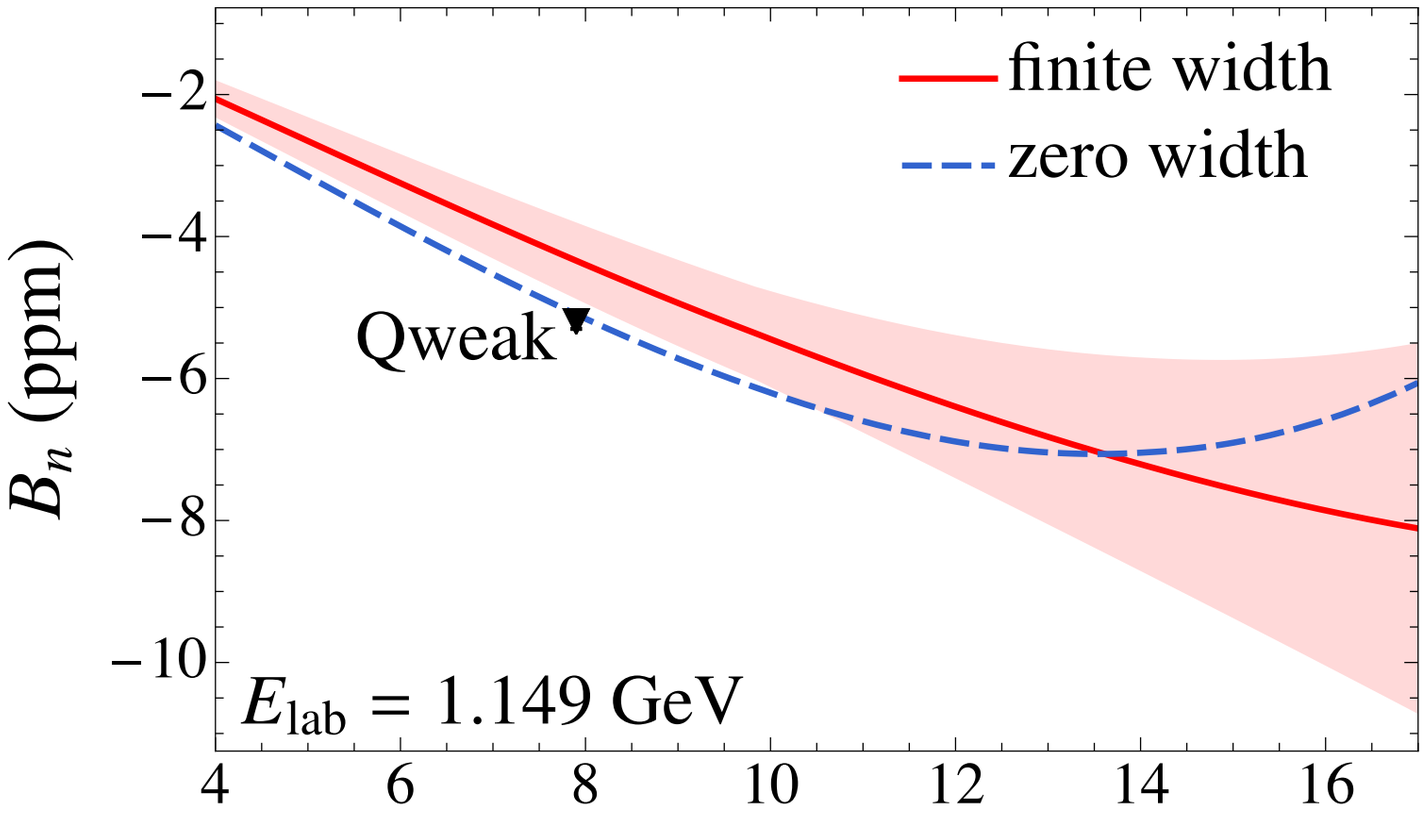

- Comparable with Afanasev and Gorchtein results
- Data point provides strong constraint on theory

Beam normal SSA: fixed θ vs E

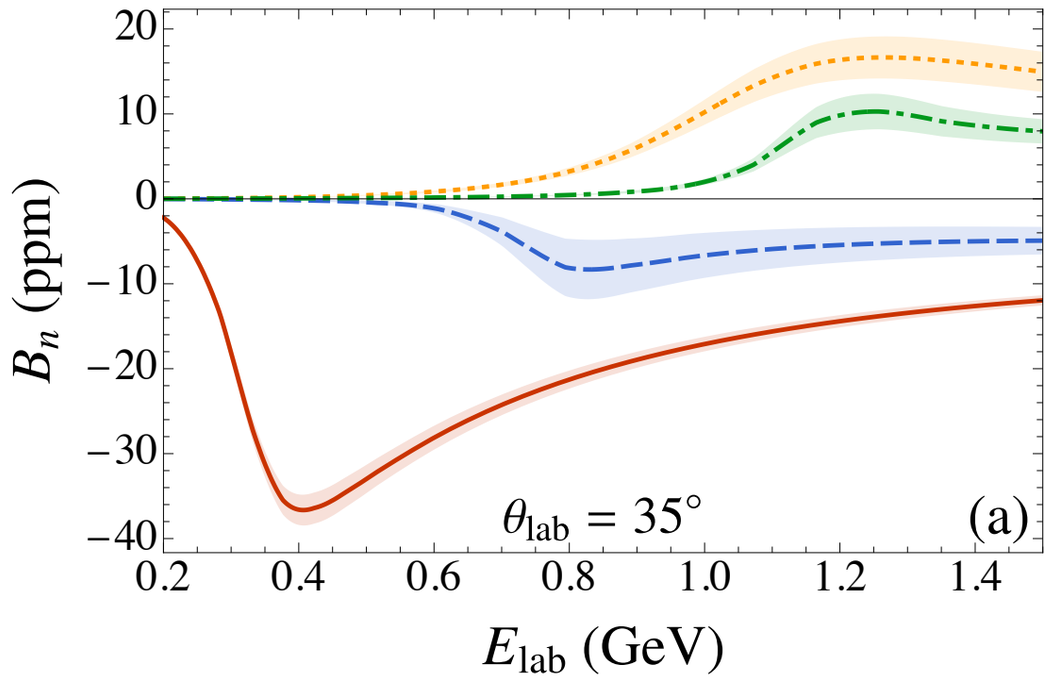

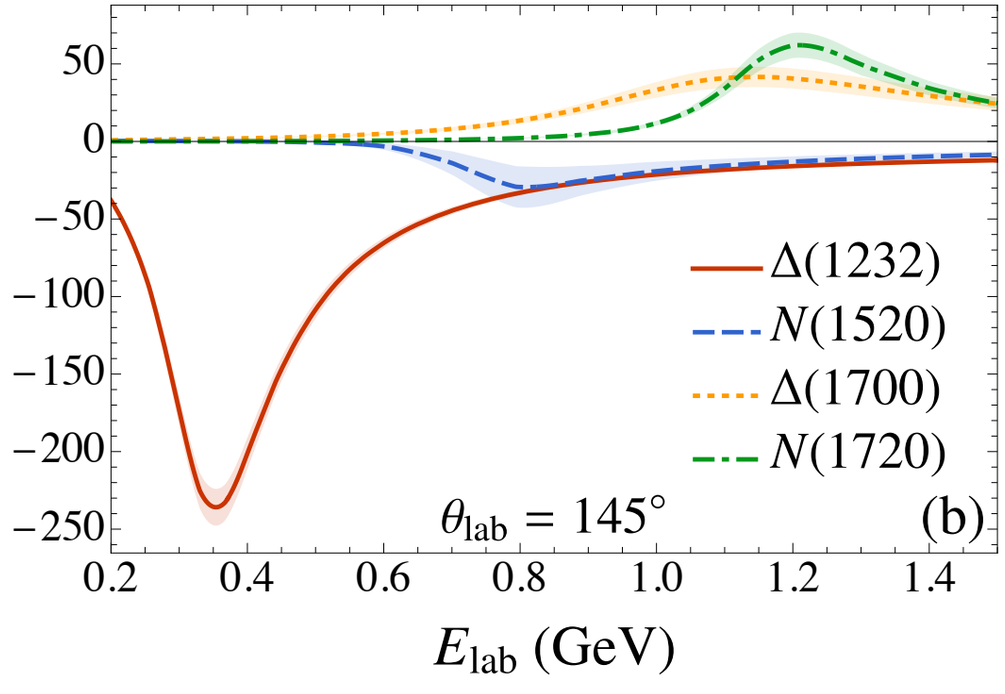

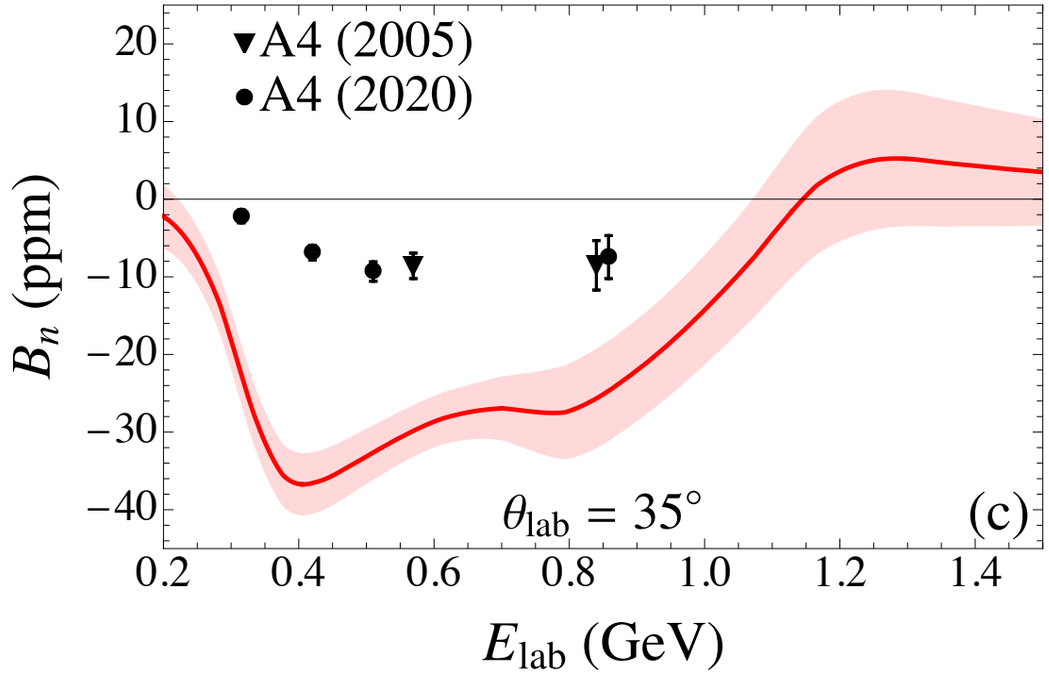

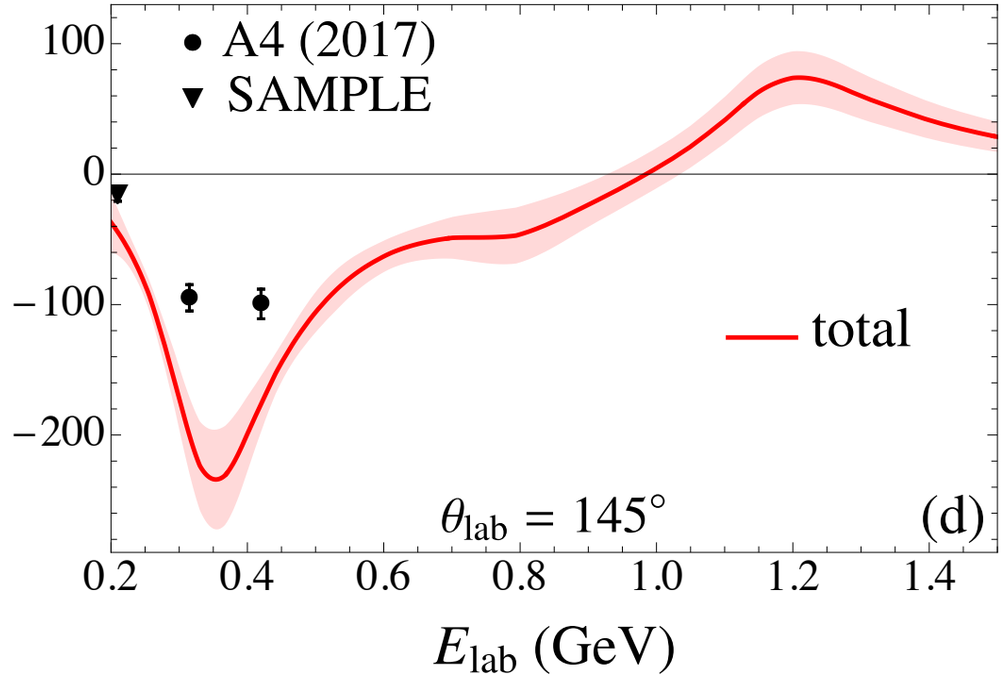

- Nominal threshold energy is at resonance peak in top row
- Tends to overshoot data in subthreshold region (low E)

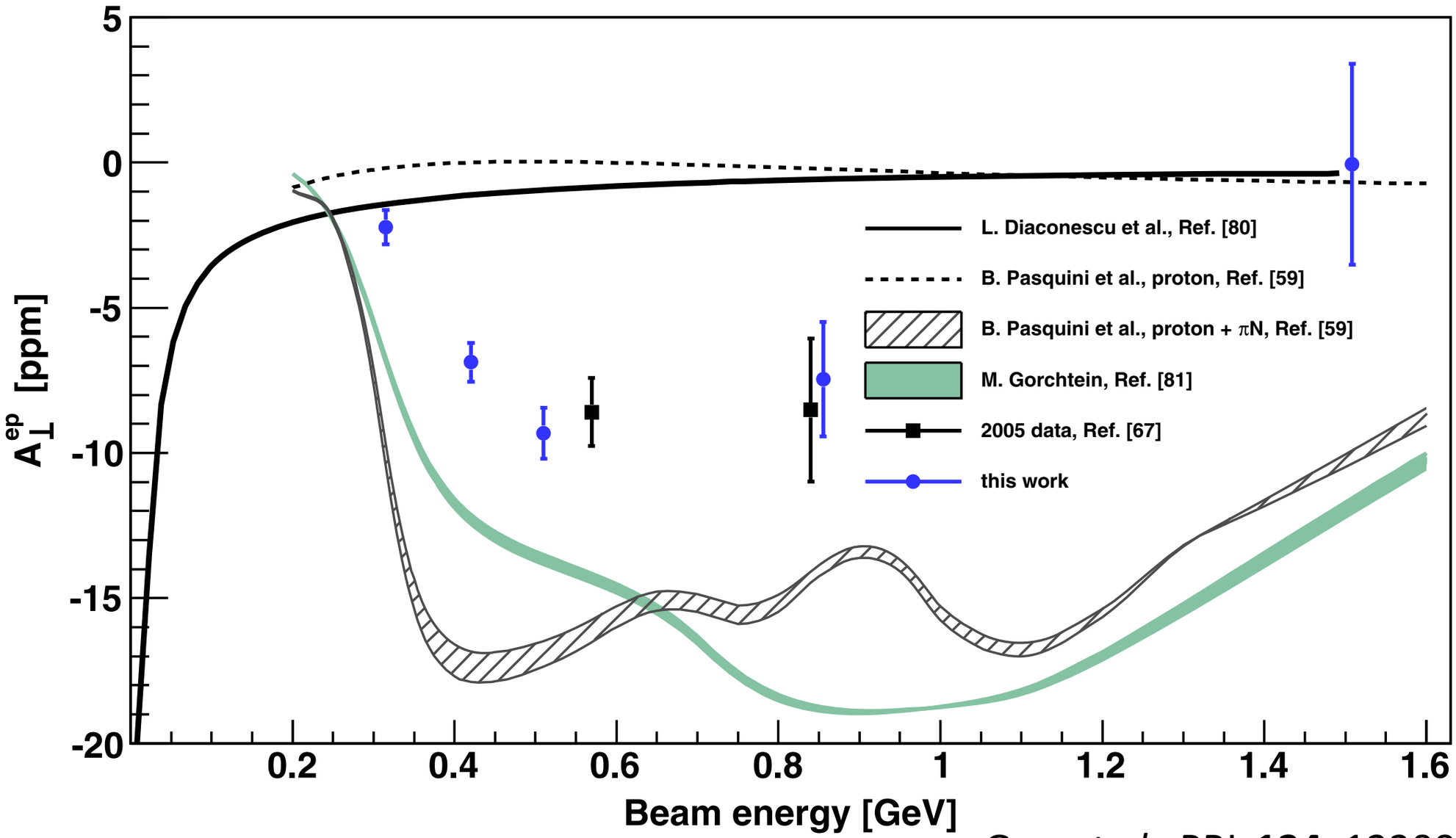

Guo *et al.*, PRL **124**, 122003 (2020)

Similar overshoot of data at low energy is seen in other work

Target normal SSA

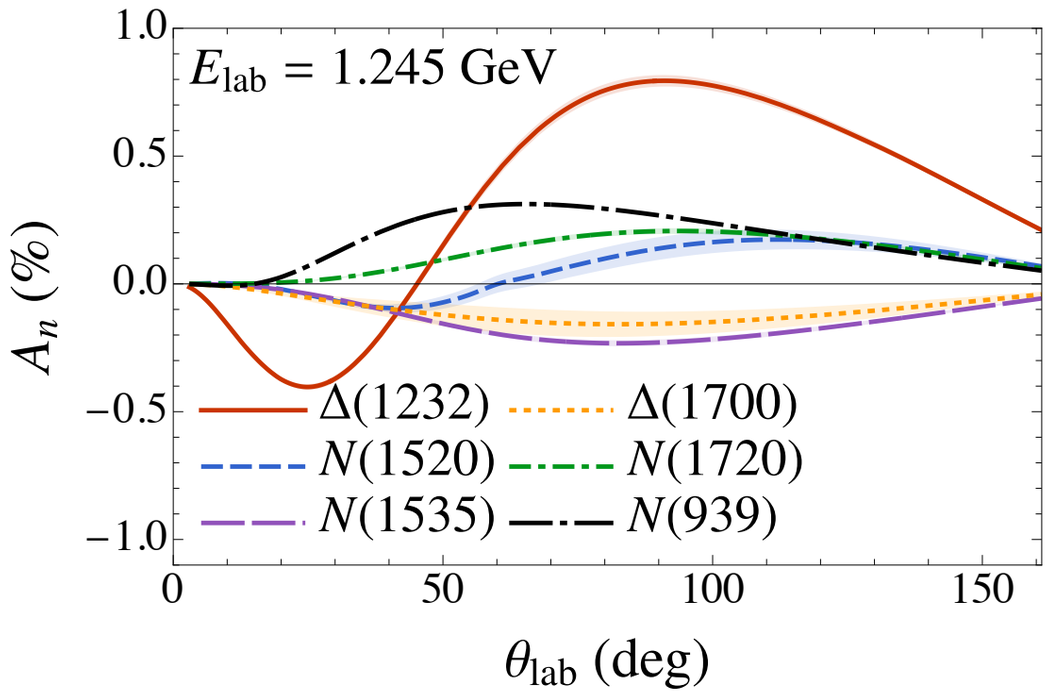

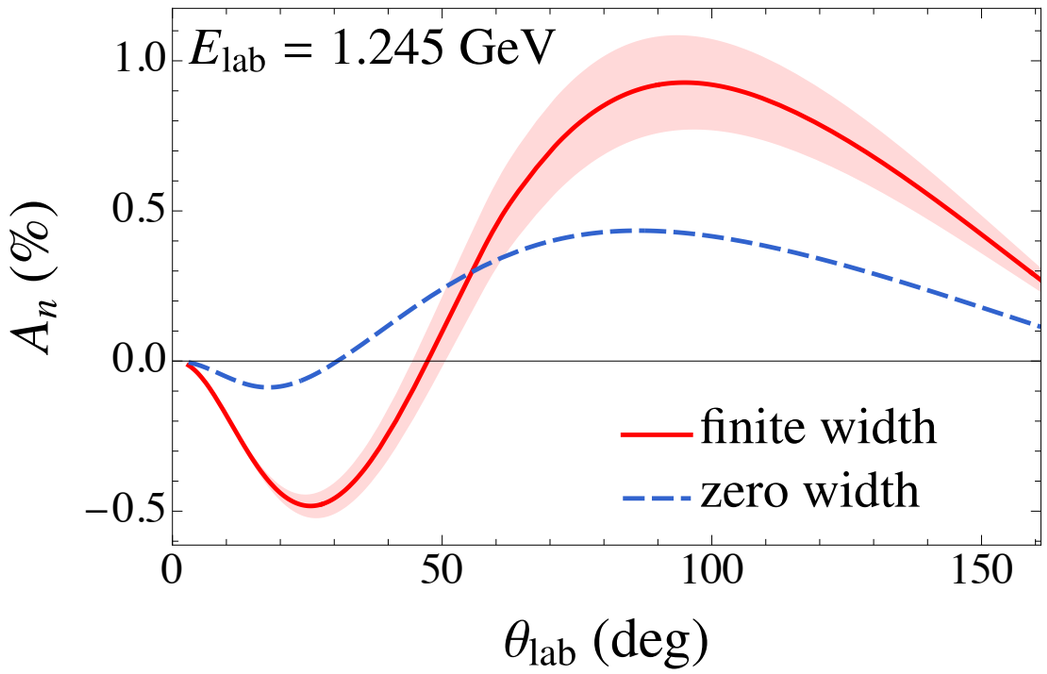

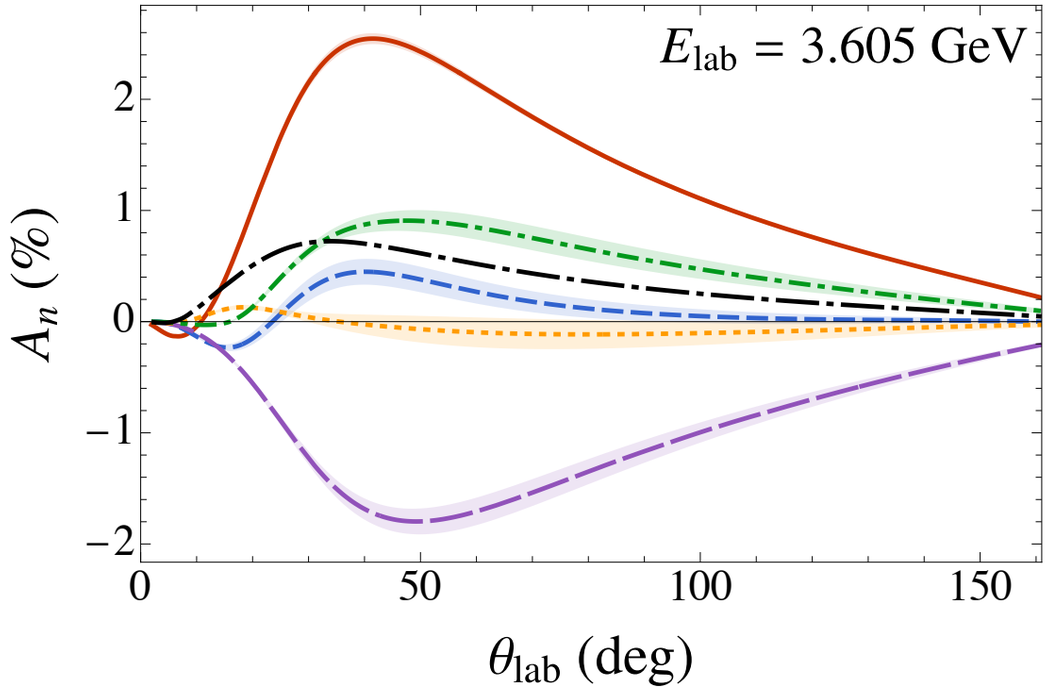

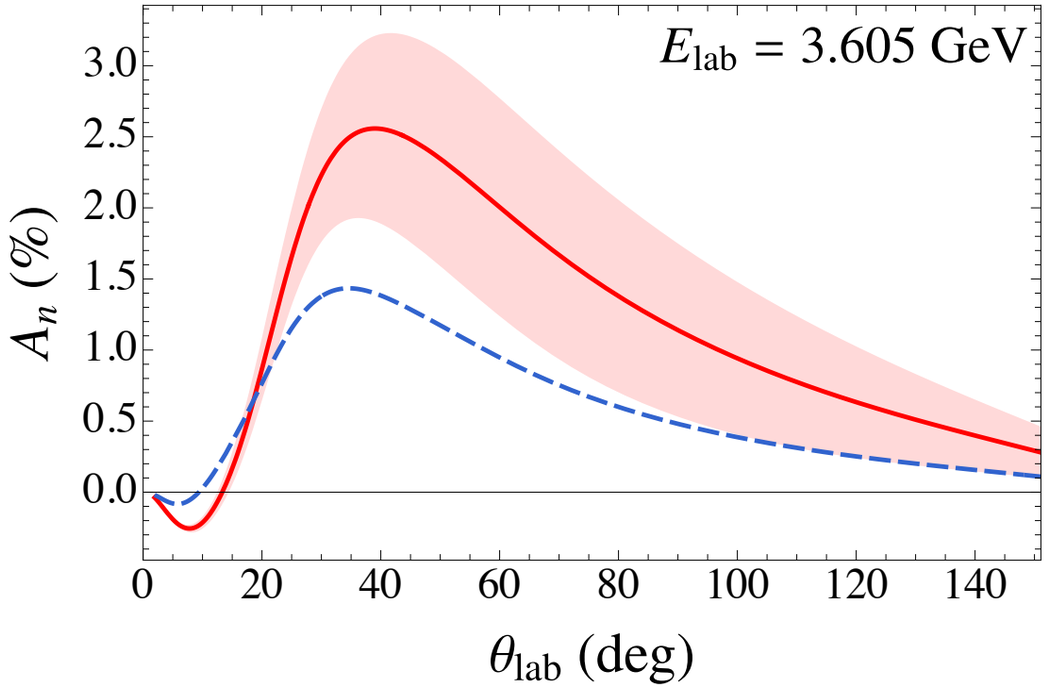

- Free of kinematics enhancements at thresholds (*i.e.* $W^2 \approx s$)
- Moderate dependence on width
- Increases as E increases (opposite of beam normal SSA)

Target normal SSA @ JLab energies

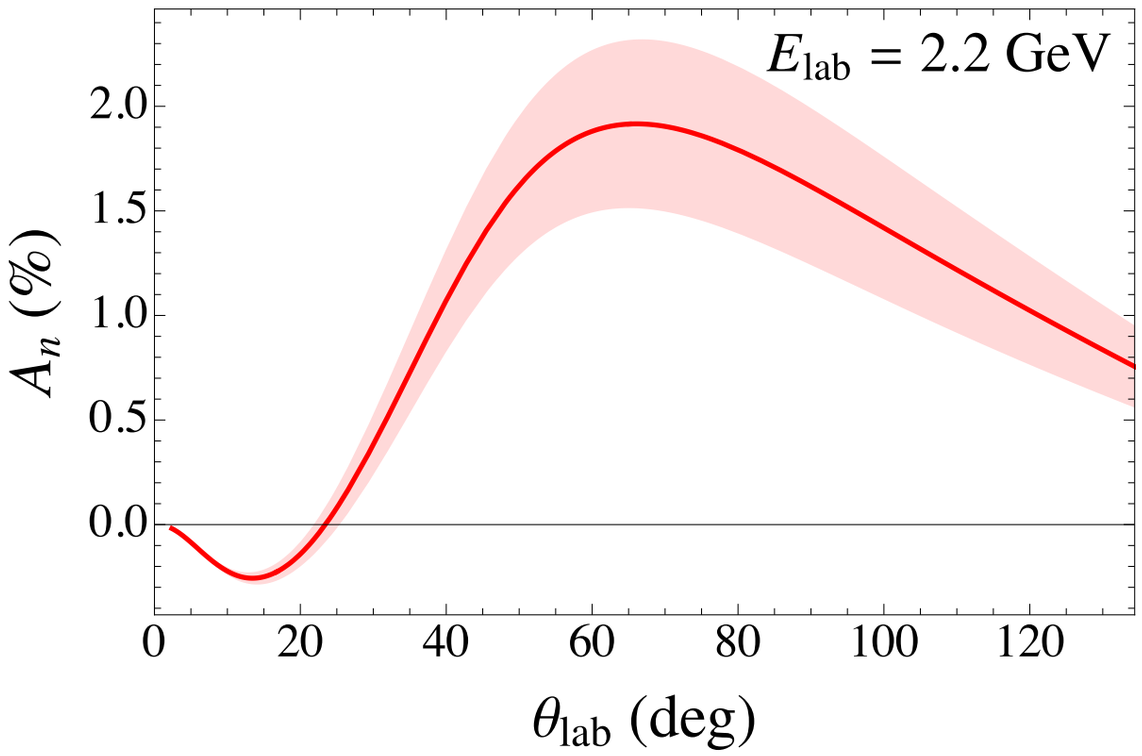

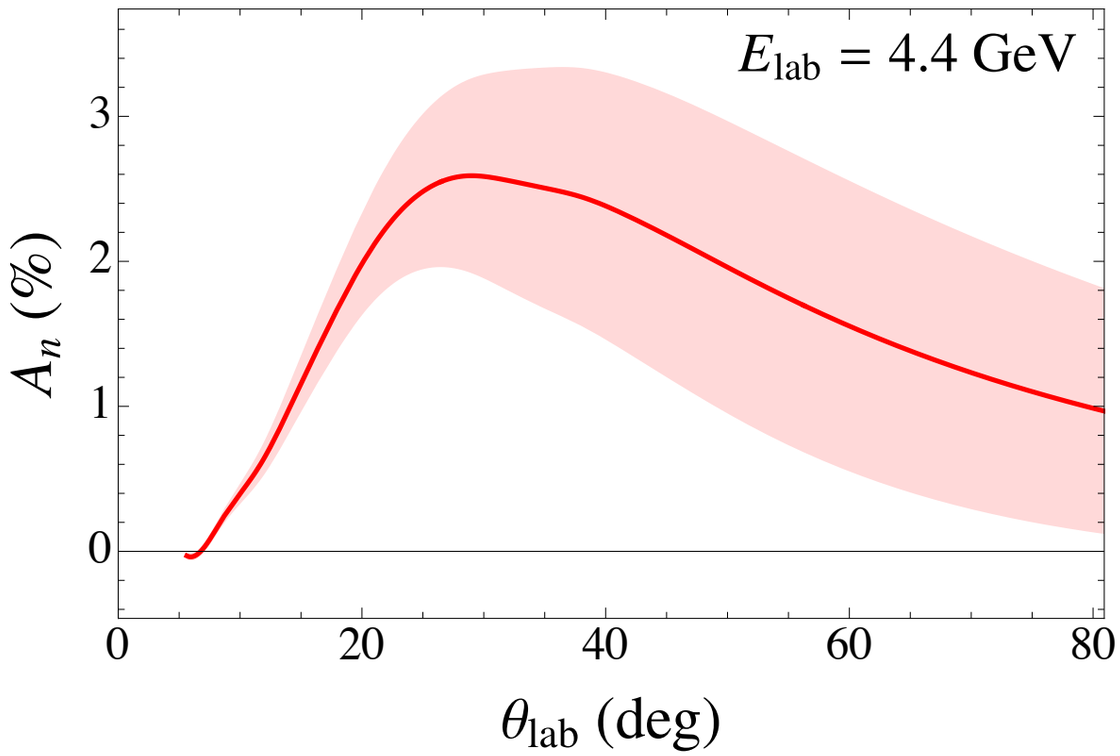

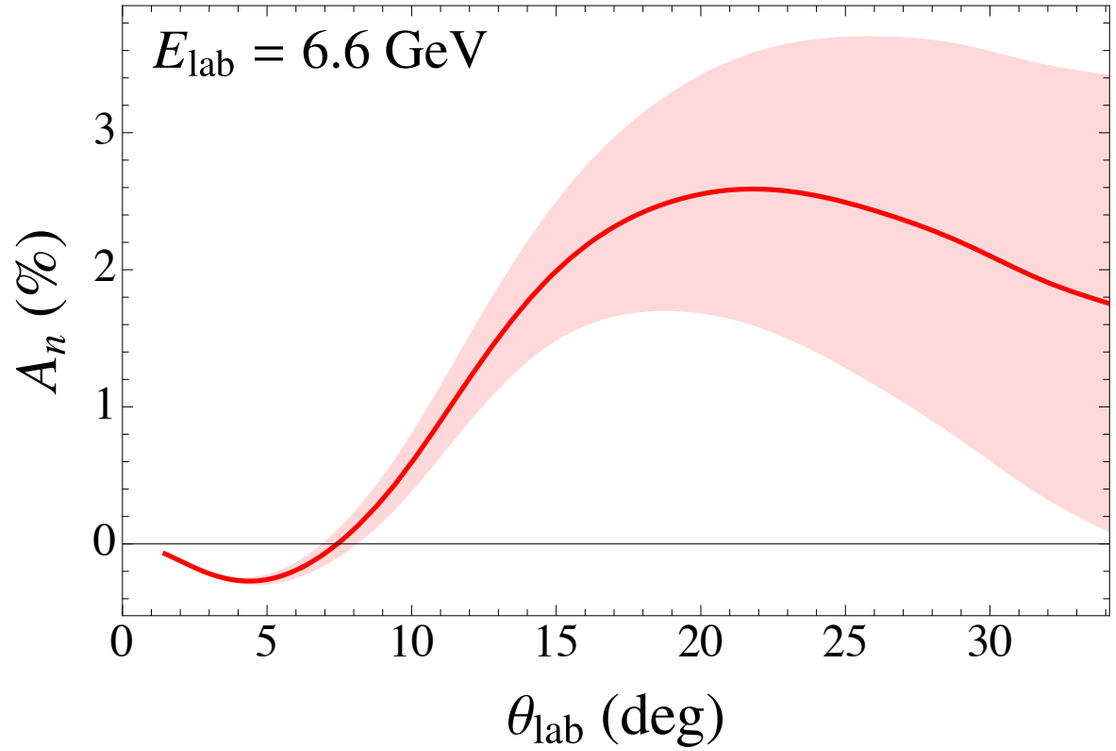

Potential 2% asymmetry in angular range 20-60° for $E_{\rm lab}$ = 2.2, 4.4, and 6.6 GeV.

Form factors and the G_E/G_M ratio

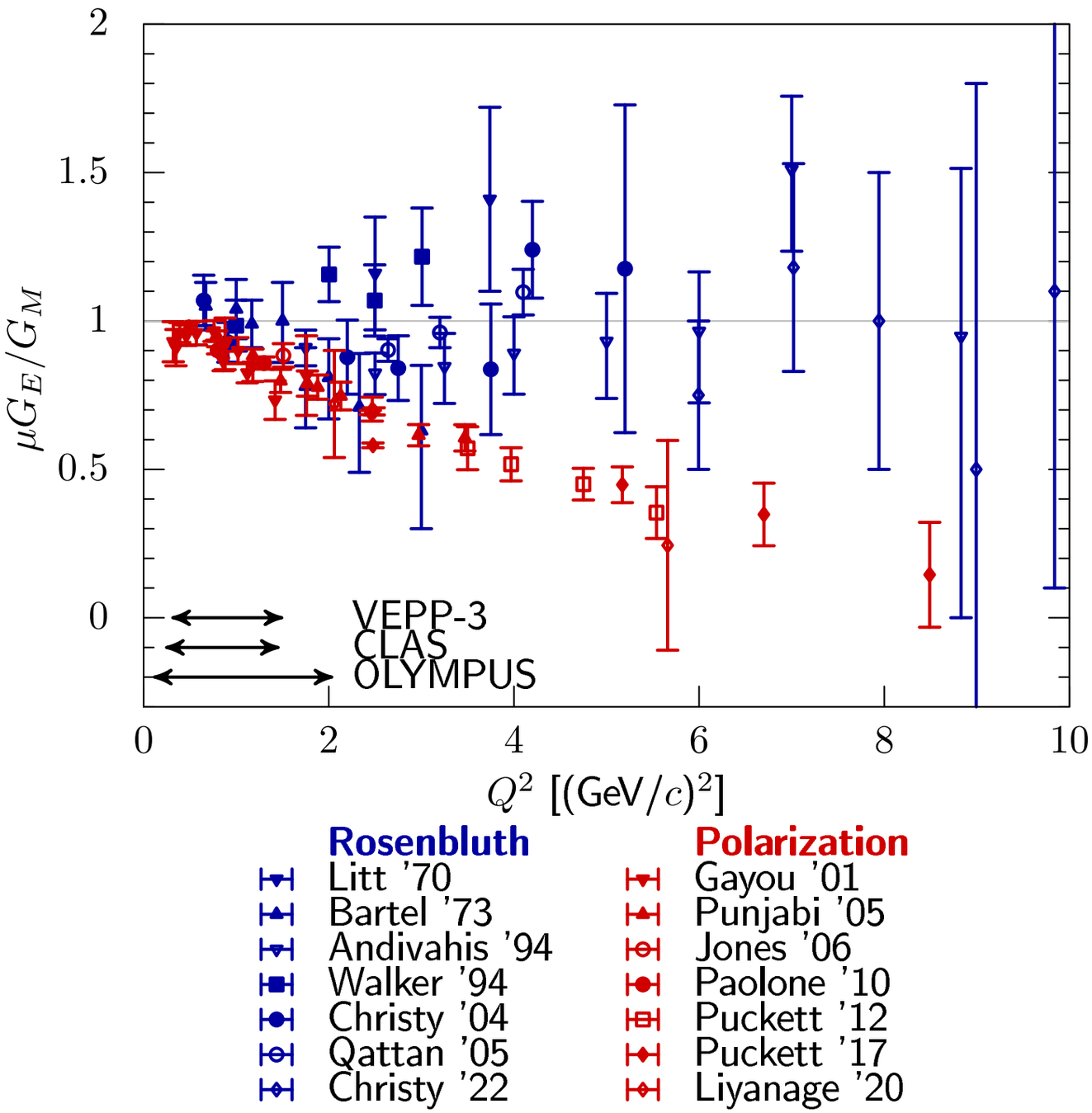

TPE leading candidate to explain discrepancy

TPE corrections to cross section (CLAS resonances)

Ahmed, Blunden & Melnitchouk, PRC**102**, 045205 (2020)

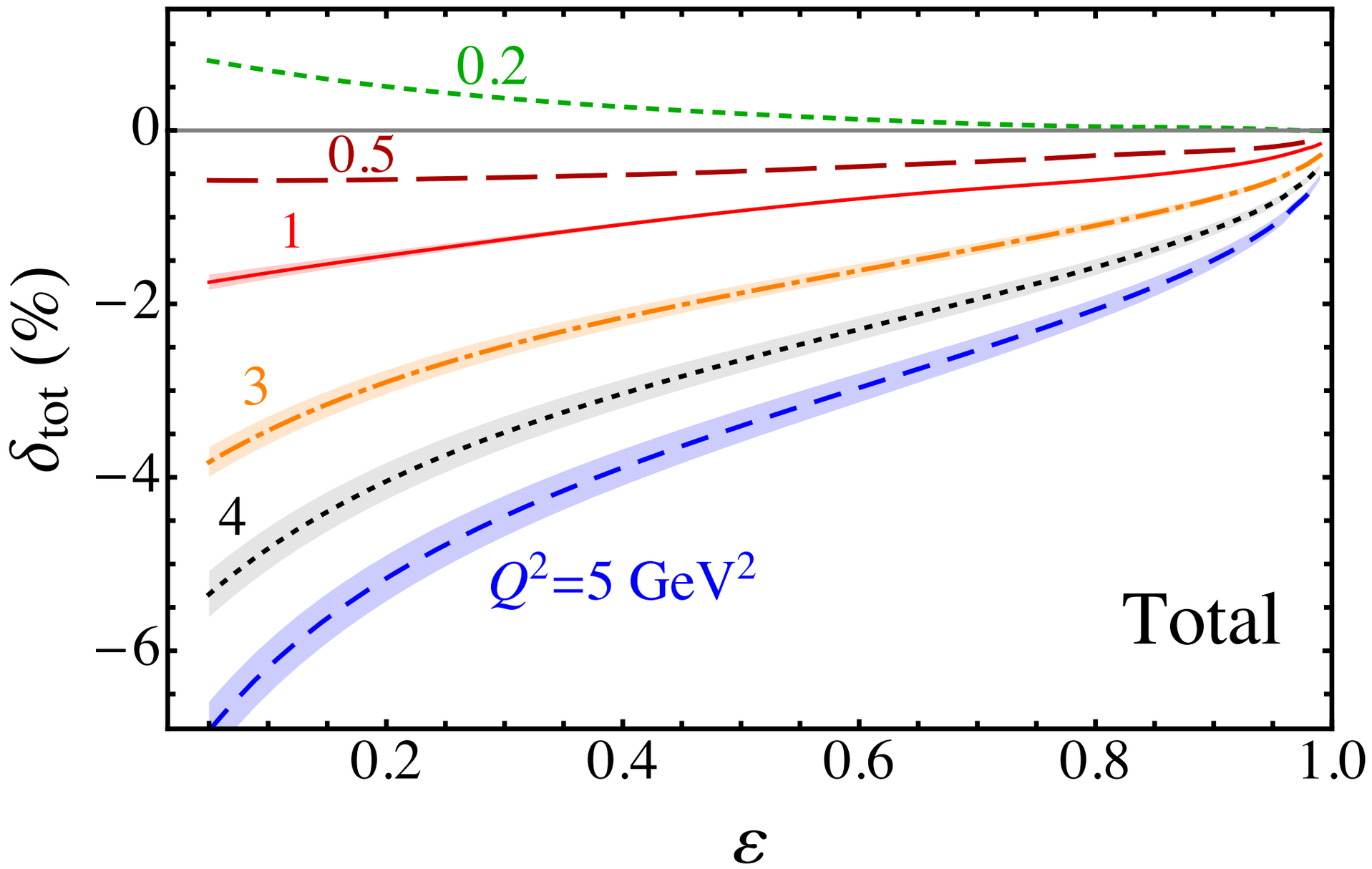

- Linear over mid-range of ε values, but curves towards endpoints
- Presence of TPE allows for smaller contribution of G_E^2 to

$$\frac{1}{\tau}\sigma_{\rm red} = G_M^2 + \frac{\varepsilon}{\tau}G_E^2$$

$$\frac{1}{\tau}\sigma_{\rm red} = G_M^2 + \frac{\varepsilon}{\tau}G_E^2$$

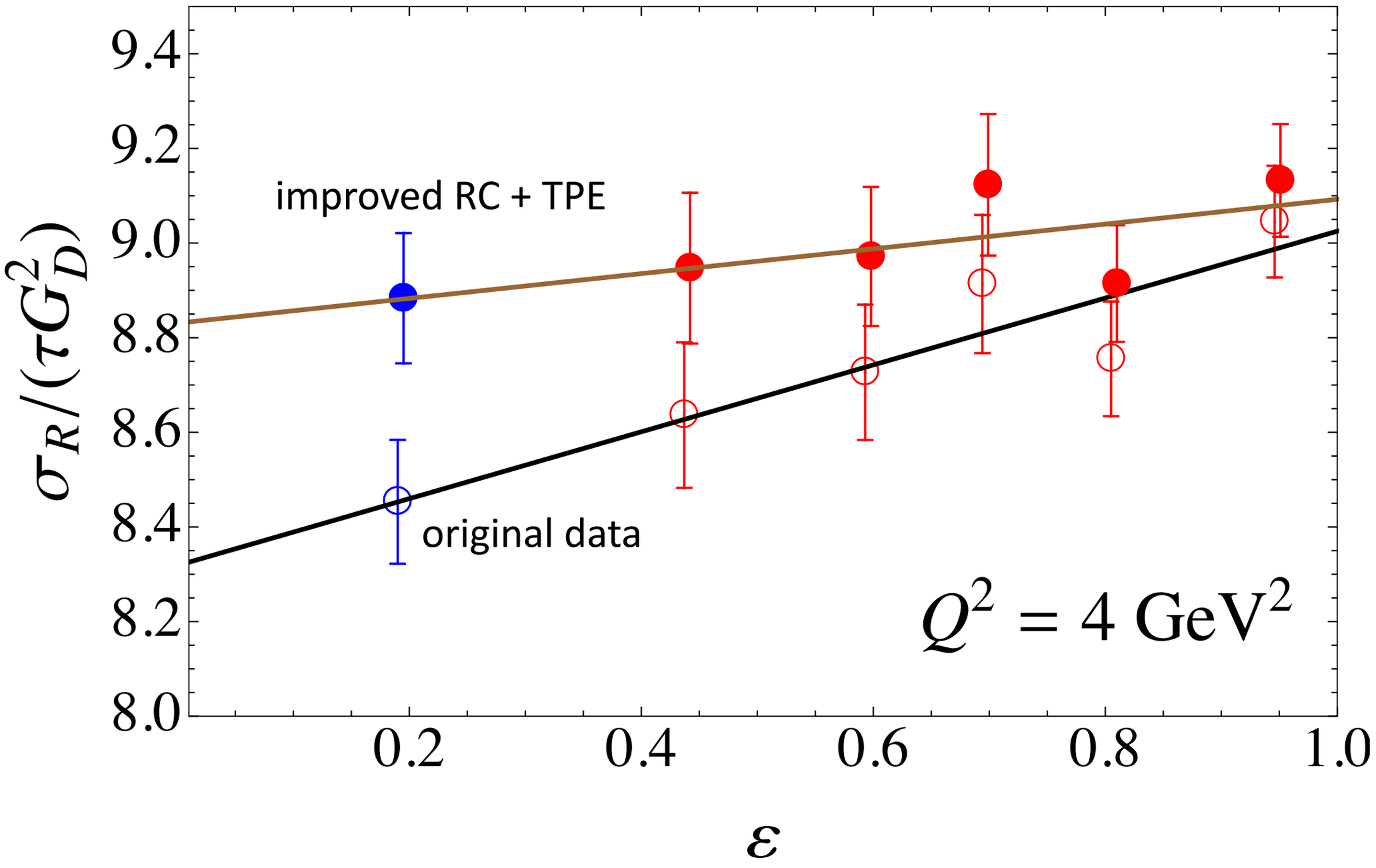

- Example from Andivahis data set at $Q^2 = 4\ \mathrm{GeV}^2$
- Uses improved RC + our TPE
- No evidence of non-linearity

Summary

- Beam normal SSA: interesting and challenging
  - dominated by spin $3/2$
  - mutual cancellation between opposite parities
  - seems to overestimate data at low energies (where $\Delta(1232)$ dominates) and underestimate data at high energies
- Target normal SSA: lack of data
  - Imaginary part of same generalized form factors as for cross section (real) — connected by dispersion relations
  - Potential 2% asymmetry at JLab energies 2.2 to 6.6 GeV and angles from $60°$ to $20°$